

Critical Bursts in Filtration

Filippo Bianchi,^{1,*} Marcel Thielmann,^{2,†} Lucilla de Arcangelis,^{3,‡} and Hans Jürgen Herrmann^{1,§}

¹*Computational Physics for Engineering Materials, Institute for Building Materials, ETH Zürich, 8093 Zurich, Switzerland*

²*Bayerisches Geoinstitut, University of Bayreuth, 95440 Bayreuth, Germany*

³*Department of Industrial and Information Engineering, University of Campania Luigi Vanvitelli, 81031 Aversa (CE), Italy*



(Received 14 September 2017; published 19 January 2018)

Particle detachment bursts during the flow of suspensions through porous media are a phenomenon that can severely affect the efficiency of deep bed filters. Despite the relevance in several industrial fields, little is known about the statistical properties and the temporal organization of these events. We present experiments of suspensions of deionized water carrying quartz particles pushed with a peristaltic pump through a filter of glass beads measuring simultaneously the pressure drop, flux, and suspension solid fraction. We find that the burst size distribution scales consistently with a power law, suggesting that we are in the presence of a novel experimental realization of a self-organized critical system. Temporal correlations are present in the time series, like in other phenomena such as earthquakes or neuronal activity bursts, and also an analog to Omori's law can be shown. The understanding of burst statistics could provide novel insights in different fields, e.g., in the filter and petroleum industries.

DOI: [10.1103/PhysRevLett.120.034503](https://doi.org/10.1103/PhysRevLett.120.034503)

The filtration of fluids through deep bed filters is a problem of great technological interest due to the wide range of related applications, such as the purification of liquid aluminum for can construction, the design of self-regenerating filters, or the prediction of sand production in oil wells. Experimentally, it has been shown that, depending on local flow conditions, bursts appear in fluid flow and pressure drop across the filter [1–3], which represent an important problem affecting the efficiency and lifetime of the filter itself. Despite the relevant technological impact of bursts, no attention has been given so far to a detailed statistical analysis of their occurrence. Such an analysis is of great importance, since information about the range of burst sizes and their temporal organization can help the optimization of filter performance. We therefore experimentally address this problem in order to measure and analyze statistical properties of long time series of bursts.

A number of microscopic mechanisms is responsible for the deposition and resuspension of particles leading to bursts. Particle deposition reduces filter porosity and permeability, and it occurs through particle interception by the filter matrix, inertial impaction of suspended particles against the matrix, Brownian diffusion, and gravity [4–6]. Upon contact, small particles ($< 10^1 \mu\text{m}$) stick to the filter matrix surface because of van der Waals forces [4–6], whereas larger particles are mainly retained by mechanical clogging due to particle straining and bridging in pore throats [4,7]. Conversely, fluid-flow-induced drag forces are responsible for particle detachment, as soon as they exceed the adhesive forces between the particle and the filter matrix or deposit [8,9]. In order to observe particle resuspension [8,10], it is necessary to

achieve a certain value of fluid velocity, which is then enhanced if flow surges occur [11,12]. Detachment is also favored by instabilities caused by suspended particles [13] that hit and detach previously deposited particles or pore pressure fluctuations due to the passage of other particles close by [14]. Resuspended particles can then either be reentrapped in deeper filter layers or exit the filter with the effluent [8,15].

Experimental investigations have shown that a dynamic equilibrium can be reached between deposition and detachment rates [1]. Such an equilibrium corresponds to morphological modifications inside the filter [16] caused by the plugging and unplugging of pores. This effect becomes visible as bursts, i.e., fluctuations either in the solid fraction (ratio between the volume of solid particles and the total volume) of the effluent [1] or in the differential pressure or else in the permeability through the filter [2] (which is observed at the field scale in oil reservoirs [3]). Several models have therefore been developed to take into account the deposition and detachment of particles (see, e.g., Refs. [17–23]). In this study, we characterize the statistical properties of burst sizes by experimentally generating long time series. We also question the existence of temporal correlations between events which could lead to a sequence of close-in-time bursts seriously affecting the filter.

We measure the flow of a Newtonian aqueous suspension of quartz particles (whose size is large enough for Brownian motion to be negligible) through a densely packed filter bed of glass beads (see Fig. 1 and Supplemental Material [24] for details). The closed loop design of our setup allows us to perform long-term experiments and, thus, to collect the long data series necessary to

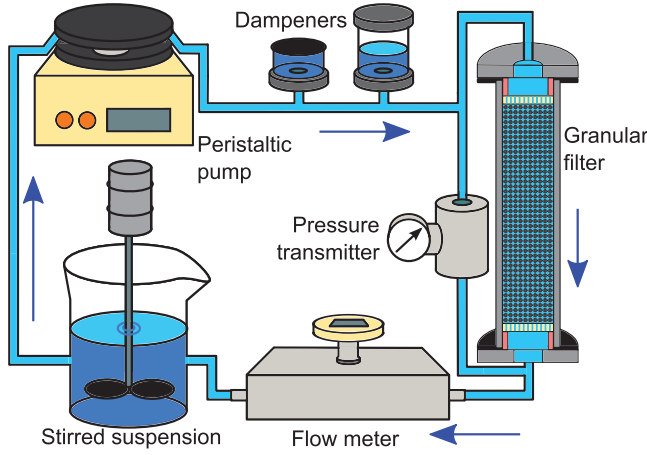


FIG. 1. Experimental setup. The suspension is pumped from a beaker through two pressure oscillation dampeners and through the granular filter.

perform a reliable statistical analysis. In a certain range of experimental parameters, we observe permeability jumps which are related to particle resuspension bursts inside the filter.

Filtration regimes.—The clogging behavior of the filter is strongly influenced by the solid fraction $[\Phi = (\rho - \rho_w)/(\rho_s - \rho_w)]$, where ρ is the suspension density, ρ_w the water density, and ρ_s the quartz density], whereas the flow rate Q has a negligible effect (see Fig. 2). Three different regimes are identified: a nonclogging regime, a clogging regime, and an intermediate transient regime.

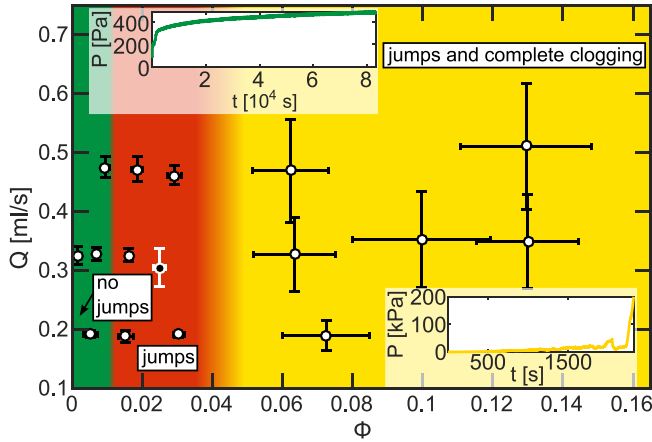


FIG. 2. Filter phase diagram. At low solid fractions, the flux is continuous with no indications for clogging (green area). With an increasing solid fraction, jumps are observed (red area). For even higher values of Φ , the filter reaches complete clogging (yellow area). Every point in the diagram indicates an experiment, and error bars represent variations of Q and Φ ($\pm 1.96\sigma$, where σ is the data standard deviation). The black point with white error bars indicates the parameters of the experiments whose statistical analysis is shown in the following. The insets show the typical pressure loss vs time evolution for experiments of the non-clogging (upper inset) and clogging regime (lower inset).

At low solid fractions ($< 10^{-2}$), pressure loss through the filter ($P = P_1 - P_2$, where P_1 and P_2 are the pressures at the filter inlet and outlet, respectively) rises very slowly, approaching asymptotically a constant (upper inset in Fig. 2). No significant fluctuations are observed, indicating that deposition does not play an important role and that particle detachment bursts are absent.

Experiments performed with a suspension solid fraction larger than 10^{-2} show a series of pressure loss jumps and, thus, in permeability. If Φ is smaller than 4×10^{-2} , complete clogging does not occur. The overall rise of pressure loss is very slow (3×10^4 Pa in more than 4 days for the experiments shown in Fig. 3). This implies that experiments are close to a steady state, in which the mean value of P is stationary and fluctuates only due to pressure loss jumps. This is an indication of a dynamical competition between deposition and resuspension inside the filter.

If Φ is increased above $\approx 5-6 \times 10^{-2}$, pressure loss jumps are still observed during the experiments (lower inset in Fig. 2). In this case, the filter permeability reduction is so strong that complete clogging is reached and fluid flow through the filter stops completely.

Resuspension bursts.—Here we analyze three experiments run under the same experimental conditions (Fig. 2) in the transient regime for about 4.5 days. The temporal evolution of the pressure loss, the flow rate, and the suspension solid fraction are measured as a function of time (Figs. 3 and 4).

Figure 3 shows that P increases in time with a sequence of successive jumps which can be attributed to particle deposition inside the filter. The time evolution of the flow rate also exhibits jumps, which occur at the same time as the pressure loss jumps (Fig. 4). Indeed, the flow rate increases at the beginning of a jump, reaches a maximum, and then decreases to its initial value (inset in Fig. 4). At the same time, the suspension solid fraction follows the same

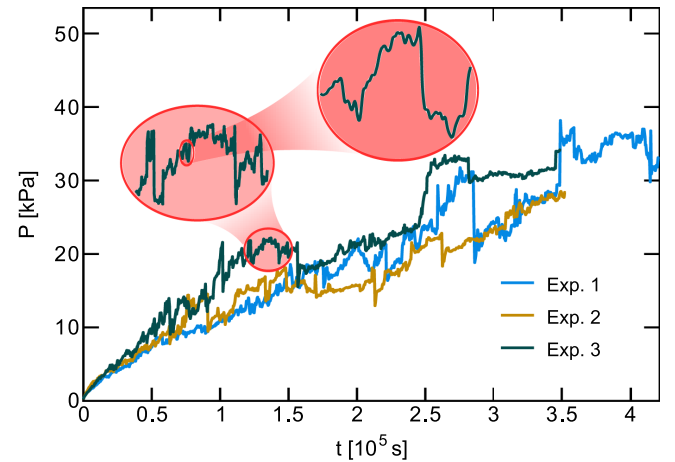


FIG. 3. Time evolution of pressure loss P through the filter during three experiments. Successive enlargements into a temporal interval are shown in the balloons.

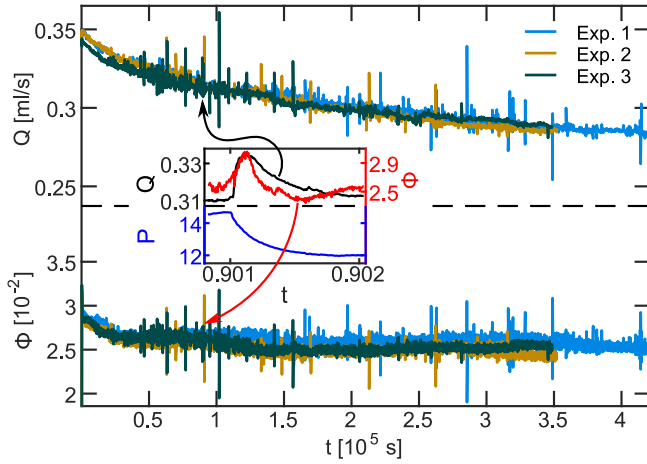


FIG. 4. Time evolution of the flow rate Q and the suspension solid fraction Φ during the three experiments. The inset shows the temporal evolution of Q and Φ (top) and P (bottom) during a single jump of experiment 3 indicated by the arrows (units are the same as in the main figure, and P is in kPa).

behavior as the flow rate, with a faster decay to the initial value.

The fact that Q increases together with pressure loss jumps implies that the sample permeability increases as well, which can be explained by the opening of new channels due to resuspension of previously deposited particles. The frequent occurrence of these jumps indicates that experiments are characterized by a continuous interplay between deposition phases and detachment bursts. When P increases, deposition dominates and pores in the filter become increasingly clogged. Consequently, local flow rates in the individual pores increase. As soon as a sufficient flow rate is reached, particle detachment occurs, resulting in the opening of a pore. Permeability then increases, while P and the local fluid velocity decrease, thereby restarting the cycle.

We compute the jump abruptness as the ratio between pressure loss jump size ΔP and its duration τ (see Supplemental Material [24] for details on jump recognition). A log-log scatter plot of the jump abruptness $\Delta P/\tau$ vs ΔP for all data shows a linear trend (Fig. S2 in Supplemental Material [24]). Despite the scatter in the data, results are consistent for all three experiments and indicate that large jumps experience a faster decrease in pressure loss than smaller ones. A linear fit to the data suggests that jump abruptness scales as the jump size to the power of 0.73 ± 0.03 . A discussion about the mechanism behind this phenomenon can be found in Supplemental Material [24].

Size and duration distributions of jumps.—Jump sizes vary significantly during a single experiment (see Fig. 5 and Supplemental Material [24] for details), and their distributions are consistent with power laws with exponents $\alpha = 1.9 \pm 0.1$ for P , 2.4 ± 0.2 for Q , and 3.8 ± 0.3 for Φ . The exponents are computed by applying the maximum

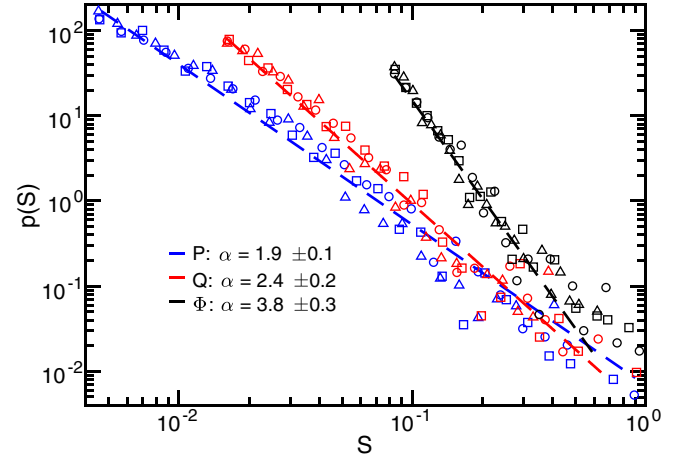


FIG. 5. Size distribution of pressure loss (blue), flow rate (red), and solid fraction (black) jumps. Circles are data from experiment 1, triangles from experiment 2, and squares from experiment 3. The jump size S is normalized by the size of the largest jump. The error of the exponents α is evaluated as the maximum difference between the fitted value for data from all experiments and from single experiments.

likelihood method [25] to data from three experiments. The power-law behavior of pressure loss jump size distribution is confirmed by the numerical simulations of Ref. [26]. Moreover, we measure the pressure loss jump size distribution by applying a smaller identification threshold (5 instead of 50 Pa; see Supplemental Material [24] for details). The power-law behavior is always retrieved with very stable exponents, implying that the absence of a characteristic size does not depend on the identification threshold. A deviation from the power-law distribution, due to the loss of events caused by the limited resolution of acquisition devices, is found only for small jump sizes. Because of experimental restrictions (such as the necessity of being in the transient regime) that do not allow a strong variation of flowing parameters, the extension of size distributions of Q and Φ is limited. Interestingly, the values of α for all three distributions are larger than the values measured for earthquakes, solar flares, and bursts in neuronal activity, which are typically in the range of 1.5–1.6 [27–29], implying that filtration belongs to a different self-organized criticality universality class.

Temporal correlations.—The consistency of size distributions with power laws suggests that, in the transient regime, filtration exhibits a scale-free behavior and that the phenomenon is critical. Beside the absence of a characteristic size, a fundamental feature of criticality is the existence of long-range temporal correlations between bursts. In order to verify their existence, we calculate the pressure loss jump rate μ (over nonoverlapping windows of 5000 s) as a function of the time for each experiment (Fig. 6). We observe that μ is not a constant, as one would expect for a perfect Poisson process. The jump rate highly fluctuates, exceeding frequently the 95% confidence

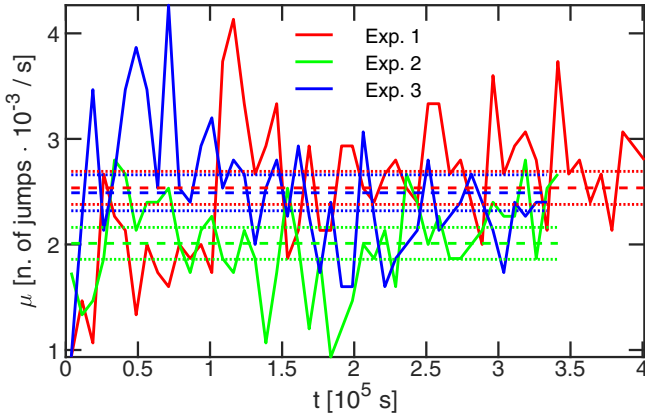


FIG. 6. Pressure loss jump rates for the three experiments. Dashed lines are the average Poissonian rates, and dash-dotted lines are the 95% confidence intervals.

intervals with respect to the average Poissonian rate for each experiment. The existence of such jumps in the rate suggests the presence of correlations in the time series.

In order to confirm the presence of correlations, we evaluate the quiet time distributions. The quiet time is the time lag between the end of a pressure loss jump and the beginning of the next one, considering only jumps larger than 150 Pa. These distributions, shown in Fig. 7(b), exhibit a more complex behavior than the exponential distribution expected for a Poisson process. Indeed, the distributions can be fitted by a Gamma function, $p(\Delta t) = 1/[B^q \Gamma(q)] x^{q-1} e^{-x/B}$ with $q = 0.84 \pm 0.04$ and $B = 1006 \pm 370$ s (the error of the fitted parameters q and B represents the maximum difference between the fitted

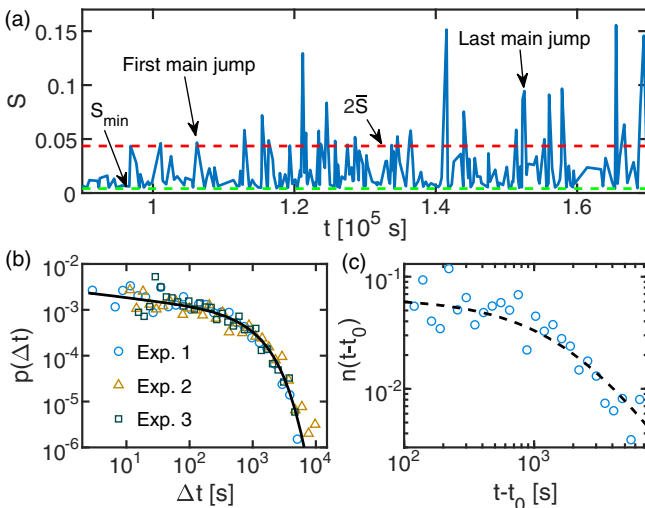


FIG. 7. (a) Jump series for experiment 1 during a phase in which μ is higher than average. Main jumps are events above the red line. The green line indicates the minimum jump size. (b) Quiet time distributions are fitted by a Gamma distribution. (c) The occurrence rate of after jumps can be fitted with the modified Omori's law.

parameters of data from all experiments and the fitted parameters of data from a single experiment). They are therefore well approximated by a power law with exponent $\beta = 1 - q = 0.16$ in an initial regime until $\Delta t \lesssim 10^3$ s, whereas for longer quiet times an exponential decay sets in. To confirm that a Gamma function represents the best fit to the data, we evaluate the Akaike information criterion for a Gamma and an exponential function. We find that the Gamma function has a lower AIC compared to the simple exponential, leading to a relative likelihood $K = e^{(AIC_{\text{gamma}} - AIC_{\text{exp}})/2} = 1.67 \times 10^{-5}$ in favor of the Gamma function. If a lower identification threshold is implemented, the quiet time distribution exhibits an exponential behavior (see Supplemental Material [24]), indicating that correlations exist mainly between large events, whereas small fluctuations in the pressure loss are dominated by uncorrelated random noise. This is a further indication that the filtration process in this regime is critical. The evidence for a Gamma function quiet time distribution is an intriguing result, since this functional behavior, with similar values of β , is common to several natural stochastic processes, such as earthquakes [27,30,31], solar flares [32,33], and acoustic emissions in rock fracture [34], where close-in-time events are temporally correlated.

Inspired by the statistical properties of seismic sequences, we investigate in deeper detail the temporal organization of events during an interval characterized by a large rate increase. We focus on the temporal sequence of events from experiment 1 between 1.1×10^5 and 1.5×10^5 s [Fig. 7(a)]. We define the main jump as a jump with size $S > 2\bar{S}$, where \bar{S} is the average jump size in the analyzed time period. Its after jumps are the following jumps occurring before the next main jump. This procedure to identify main and after events is analogous to the standard statistical analysis performed for earthquakes [27,35]. Figure 7(c) shows the number of after jumps in time, $n(t - t_0)$, occurring after a main jump occurred at $t = t_0$. We observe that $n(t - t_0)$ behaves accordingly to the modified Omori's law of earthquakes [36,37] $n(t - t_0) = A(c + t - t_0)^{-p}$ with an exponent $p = 1.8$ and a c value of 2.2×10^3 s (the parameters are estimated according to Ref. [38]). This indicates that $n(t - t_0)$ has a power-law decay with exponent 1.8 (for earthquakes, $p \approx 1$ [39]). If the data are fitted with a pure power law, the exponent is 1.4 with a smaller error bar. This result suggests that, as large earthquakes trigger a sequence of aftershocks whose rate decreases in time as a power law, large jumps trigger sequences of smaller close-in-time jumps.

Conclusions.—Our experiments show that jumps in deep bed filtration are the expression of a self-organized critical process, occurring in a regime of parameters where the balance between the deposition and detachment of particles is realized. The values of the critical exponents for the jump size distributions are different than those typically measured for other stochastic natural processes, suggesting

that this phenomenon is in a novel universality class of self-organized critical phenomena. Indeed, the absence of a characteristic event size and power-law distributions, even if with different exponents, is found in a variety of natural phenomena, such as earthquakes [27,40], solar flares [28,41], stock markets [42,43], and neural avalanches [29,44]. Therefore, the evidence for a novel universality class suggests that the microscopic mechanisms controlling the self-organization in filtration are different from all the aforementioned processes. Indeed, filtration can attain a self-organized critical state by a dynamical adjustment of the porous medium, in which the decrease or increase of the local fluid velocity reflect the resuspension or deposition of particles, respectively. This microscopic interpretation has been recently confirmed by numerical simulations that are able to reproduce the scaling behavior of the size distributions [26]. Moreover, the existence of temporal correlations between close-in-time events is evidenced by the power-law decay of the occurrence rate, similarly to Omori's law for earthquakes. These correlations between bursts confirm the relevance of hydrodynamic interactions in the process. Our results can be of interest for a number of problems where resuspension events are observed, such as, for instance, sand production in oil wells or filtration of pollutants in soil where resuspension bursts could release contaminants in the effluent.

The research leading to these results has received funding from the European Research Council, ERC Advanced Grant No. 319968-FlowCCS. We acknowledge the support of Falk K. Wittel and Claudio Madonna for helping in the design and realization of the experiments.

*fbianchi@ifb.baug.ethz.ch

†Marcel.Thielmann@uni-bayreuth.de

‡lucilla.dearcangelis@unicampania.it

§hans@ifb.baug.ethz.ch

- [1] C. Gruesbeck and R. E. Collins, *Soc. Pet. Eng. J.* **22**, 847 (1982).
- [2] M. A. Einstein and F. Civan, *J. Can. Petrol. Tech.* **31**, 27 (1992).
- [3] M. Sahimi, A. R. Mehrabi, N. Mirzaee, and H. Rassamdana, *Transp. Porous Media* **41**, 325 (2000).
- [4] J. P. Herzig, D. M. Leclerc, and P. L. Goff, *Ind. Eng. Chem.* **62**, 8 (1970).
- [5] S. Ken, *Filters and Filtration Handbook* (Elsevier, Oxford, 2008).
- [6] C. Tien, *Principles of Filtration* (Elsevier, Amsterdam, 2012).
- [7] J. R. Valdes and J. C. Santamarina, *SPE J.* **11**, 193 (2006).
- [8] R. Bai and C. Tien, *J. Colloid Interface Sci.* **186**, 307 (1997).
- [9] J. Bergendahl and D. Grasso, *Chem. Eng. Sci.* **55**, 1523 (2000).
- [10] A. Mahadevan, A. V. Orpe, A. Kudrolli, and L. Mahadevan, *Europhys. Lett.* **98**, 58003 (2012).
- [11] S. Han, C. S. Fitzpatrick, and A. Wetherill, *Water Res.* **43**, 1171 (2009).
- [12] J. Kim and D. F. Lawler, *Water Res.* **46**, 433 (2012).
- [13] K. Ives, *Water Res.* **23**, 861 (1989).
- [14] C. Ghidaglia, L. de Arcangelis, J. Hinch, and E. Guazzelli, *Phys. Fluids* **8**, 6 (1996).
- [15] J. Kim and J. E. Tobiasson, *Environ. Sci. Technol.* **38**, 6132 (2004).
- [16] A. O. Imdakm and M. Sahimi, *Phys. Rev. A* **36**, 5304 (1987).
- [17] A. Imdakm and M. Sahimi, *Chem. Eng. Sci.* **46**, 1977 (1991).
- [18] M. Sahimi and A. O. Imdakm, *Phys. Rev. Lett.* **66**, 1169 (1991).
- [19] H. A. Ohen and F. Civan, *Soc. Pet. Eng. J.* **1**, 27 (1993).
- [20] B. Ju, T. Fan, X. Wang, and X. Qiu, *Transp. Porous Media* **68**, 265 (2007).
- [21] F. Civan, *Reservoir Formation Damage: Fundamentals, Modeling, Assessment, and Mitigation* (Gulf Professional Publishing, Oxford, 2007).
- [22] J. Ochi and J.-F. Vernoux, *Transp. Porous Media* **37**, 303 (1999).
- [23] M. Sahimi, G. R. Gavalas, and T. T. Tsotsis, *Chem. Eng. Sci.* **45**, 1443 (1990).
- [24] See Supplemental Material at <http://link.aps.org/supplemental/10.1103/PhysRevLett.120.034503> for details on the experimental setup, working conditions, jump identification, jump abruptness and quiet time distribution.
- [25] M. E. J. Newman, *Contemp. Phys.* **46**, 323 (2005).
- [26] R. Jäger, M. Mendoza, and H. J. Herrmann, *Phys. Rev. Lett.* **119**, 124501 (2017).
- [27] L. de Arcangelis, C. Godano, J. R. Grasso, and E. Lippiello, *Phys. Rep.* **628**, 1 (2016).
- [28] M. Mendoza, A. Kaydul, L. de Arcangelis, J. S. Andrade, Jr., and H. J. Herrmann, *Nat. Commun.* **5**, 5035 (2014).
- [29] J. M. Beggs and D. Plenz, *J. Neurosci.* **23**, 11167 (2003).
- [30] A. Corral, *Phys. Rev. E* **68**, 035102 (2003).
- [31] A. Corral, *Phys. Rev. Lett.* **92**, 108501 (2004).
- [32] N. Crosby, N. Vilmer, N. Lund, and R. Sunyaev, *Astron. Astrophys.* **334**, 299 (1998).
- [33] M. S. Wheatland, P. A. Sturrock, and J. M. McTiernan, *Astrophys. J.* **509**, 448 (1998).
- [34] J. Davidsen, S. Stanchits, and G. Dresen, *Phys. Rev. Lett.* **98**, 125502 (2007).
- [35] L. de Arcangelis, C. Godano, E. Lippiello, and M. Nicodemi, *Phys. Rev. Lett.* **96**, 051102 (2006).
- [36] T. Utsu, Y. Ogata, and R. S. Matsu'ura, *J. Phys. Earth* **43**, 1 (1995).
- [37] I. G. Main, *Geophys. J. Int.* **142**, 151 (2000).
- [38] Y. Ogata, *J. Phys. Earth* **31**, 115 (1983).
- [39] F. Omori, *J. Coll. Sci. Imp. Univ. Tokyo* **7**, 111 (1894).
- [40] B. Gutenberg and C. F. Richter, *Bull. Seismol. Soc. Am.* **34**, 185 (1944).
- [41] E. T. Lu and R. J. Hamilton, *Astrophys. J.* **380**, L89 (1991).
- [42] P. Gopikrishnan, V. Plerou, X. Gabaix, and H. E. Stanley, *Phys. Rev. E* **62**, R4493 (2000).
- [43] M. Bartolozzi, D. Leinweber, and A. Thomas, *Physica A (Amsterdam)* **350**, 451 (2005).
- [44] L. de Arcangelis and H. J. Herrmann, in *Criticality in Neural Systems*, edited by D. Plenz and N. Ernst (Wiley-VCH Verlag GmbH & Co. KGaA, Weinheim, 2014), pp. 273–292.